

**Cell Reports, Volume 28**

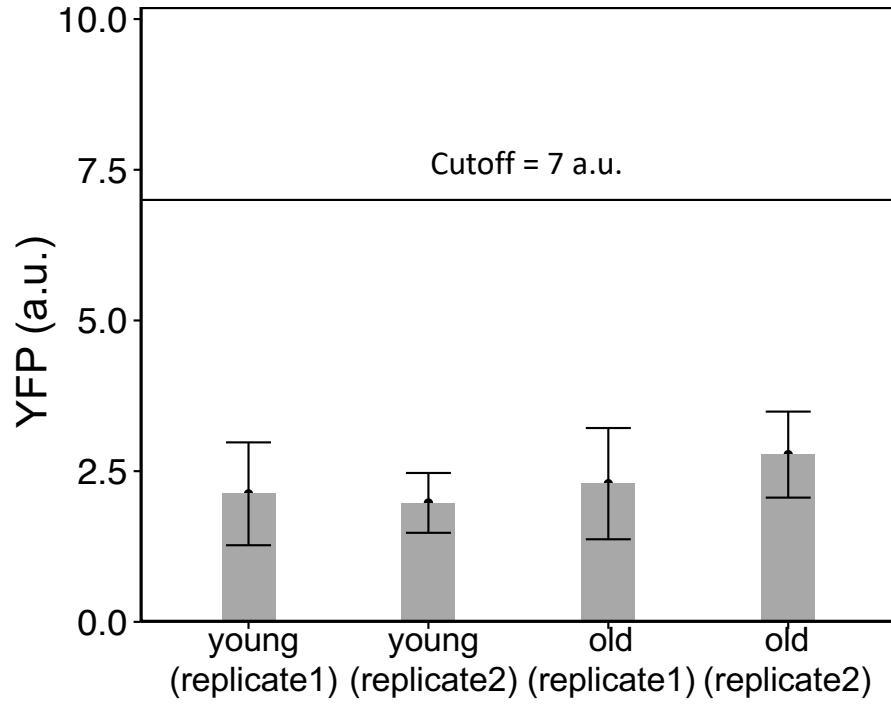
**Supplemental Information**

**Quantitative Insights into Age-Associated  
DNA-Repair Inefficiency in Single Cells**

**Thomas Z. Young, Ping Liu, Guste Urbonaite, and Murat Acar**

## I. Supplemental Figures and Legends

A



B

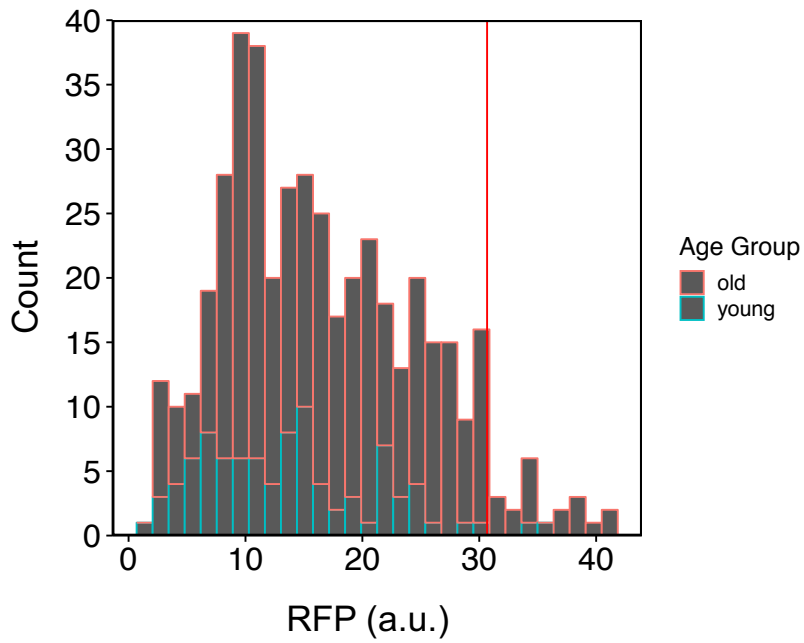


**Figure S1. A. Determination of the YFP cutoff value for SSA repair based on YFP levels in the SSA control strain without the cutsite, Related to Figures 1C, 2B.** YFP values were measured for the SSA control strain during the 140-minute time period (5 fluorescent measurements) prior to doxycycline treatment. Bar heights represent mean of the YFP measurements (in arbitrary units (a.u.)) pooled across all cells of each replicate experiment, and error bars show the standard deviation (SD). The mean + 5SD for each replicate was calculated. Mean + 5SD was 5.4 a.u. and 4.7 a.u. for the young replicates; for the old replicates, it was 6.7 a.u. and 6.4 a.u.. The horizontal line shows the cutoff level (at 7 a.u.) that was used. **B. Defining an RFP cutoff using RFP values measured from the YFP<sup>+</sup> cells of the SSA+RFPdegron strain (yTY147a), Related to Figure 3A.** The histogram shows the distribution of all RFP measurements over the first 12 hours of the movie, for cells that initially were strongly YFP<sup>+</sup> (YFP > 300 a.u.). Bars are color coded to show the counts of measurements from each age group. The red vertical line corresponds to the 95% quantile of this distribution, which was used as the RFP cutoff.

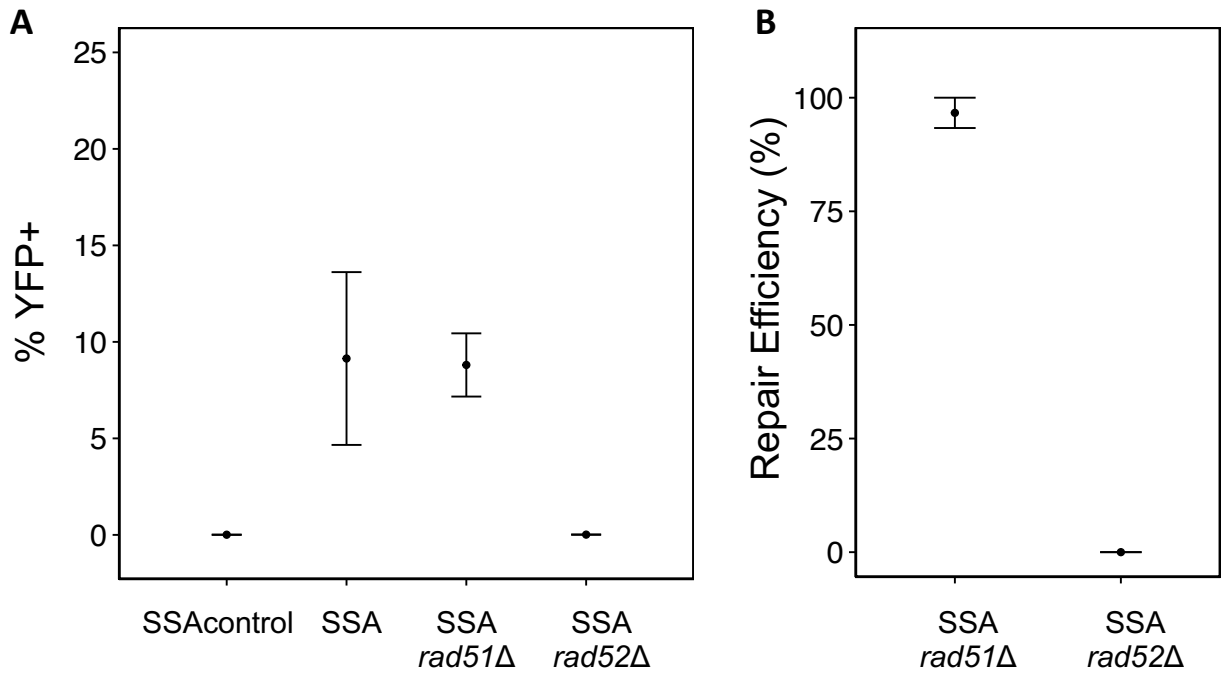


**Figure S2. Assessing the dependence of the SSA repair reporter on DNA repair proteins Rad51 and Rad52, Related to Figures 1C, 2B.** All strains contained the perfect homology SSA reporter. **A.** Percentage of YFP<sup>+</sup> (repaired) cells in overnight-grown cultures. No doxycycline was added, so any repaired cells are the product of leaky cutting by I-SceI (leaky activity of the promoter driving I-SceI). The SSAcontrol strain is identical to the SSA strain except that it lacks the I-SceI cutsites. The strains deleted in *RAD51* and *RAD52* genes have the same reporter as the SSA strain. For each strain, the mean $\pm$ SEM of YFP<sup>+</sup> percentages for 4 cultures is plotted. **B.** SSA repair efficiency after DSB induction in young cells of the strains deleted in the *RAD51* or *RAD52* genes. Error bars correspond to mean $\pm$ SEM (n=2) of replicate based repair efficiencies. The data was obtained using the microscope movie protocol for the young age-group described in the STAR Methods section named ‘DSB induction experiments in aging cells’. Since deleting *RAD51* or *RAD52* genes reduces the replicative lifespan, old cells ( $\geq 15$  generations) were not observable.

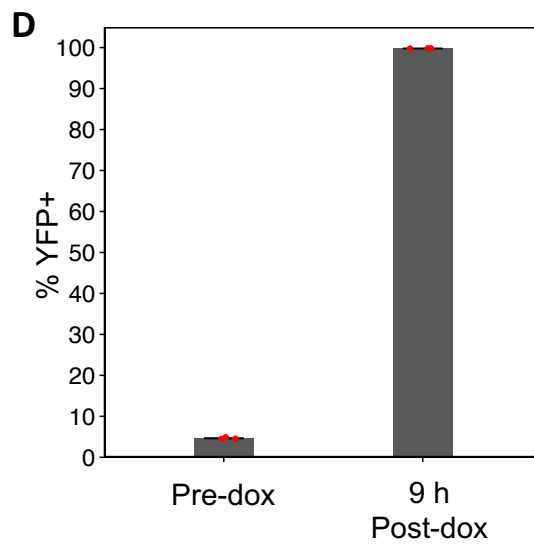
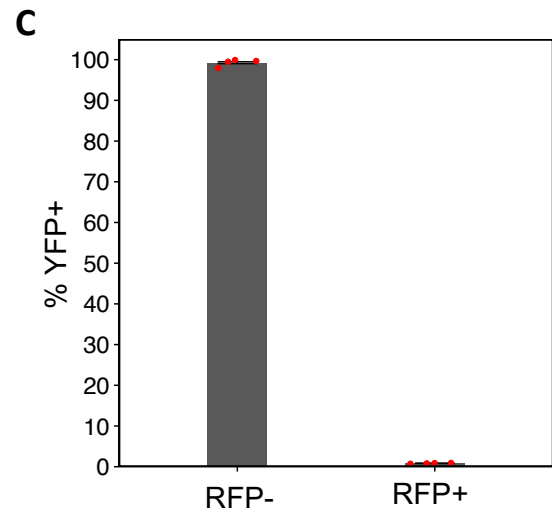
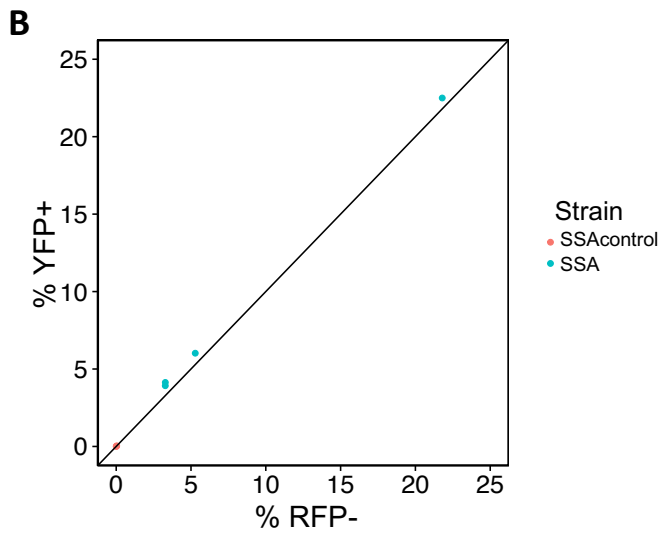
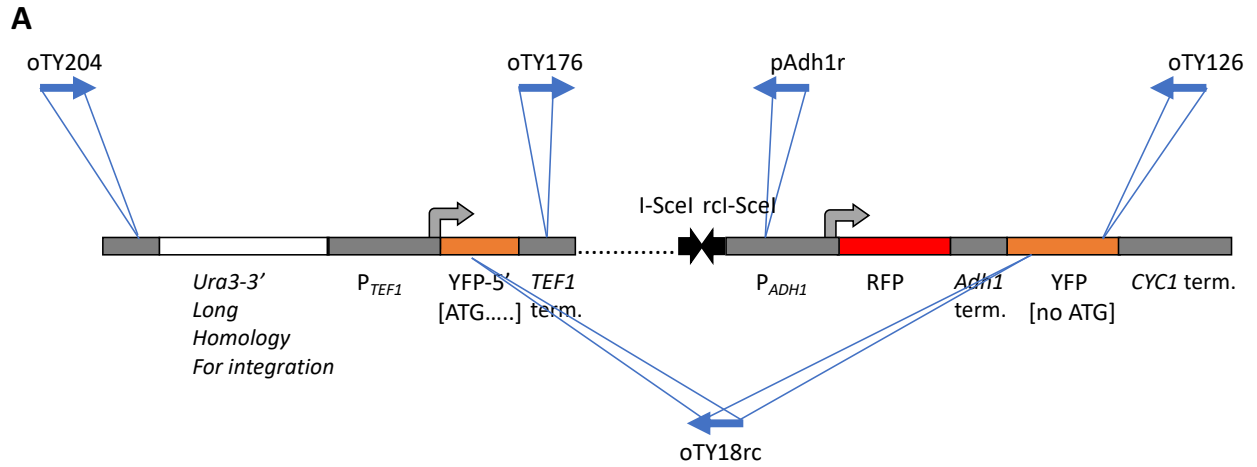


**Figure S3. A. Primers for characterizing the genomic sequence at the locus carrying the SSA reporter (following doxycycline expression in cultures), Related to Figure 1C.** Results are shown in Table S1. A description of the primers and PCR products is given in the STAR Methods section named ‘Sequencing-based genotypic characterization of the SSA reporter activity’. The primer sequences can be found in the Key Resources Table. **B-D. Characterization of the sensitivity of the YFP-based SSA reporter to SSA repair events, Related to Figure 1C.**

**B.** YFP<sup>+</sup> and RFP<sup>-</sup> percentages of cells in overnight-grown cultures agree. Percentage of YFP<sup>+</sup> cells vs percentage of RFP<sup>-</sup> cells for overnight-grown cultures of SSA (n=4) and SSAcontrol (n=4) strains is plotted. No doxycycline was added to cultures, so the SSA-positive fractions are due to leaky I-SceI expression and cutting, followed by SSA repair. The diagonal line passing through (%RFP<sup>-</sup> = 0; %YFP<sup>+</sup> = 0) with slope 1, is what would be expected if YFP occurs if and only if RFP is absent. The percentages of RFP<sup>-</sup> and YFP<sup>+</sup> cells in all four overnight-grown SSAcontrol-strain cultures overlap around 0%. Results from two of the overnight-grown SSA-strain cultures overlap around an RFP<sup>-</sup> and YFP<sup>+</sup> percentage of 4%. **C.** Nearly all SSA repair events due to leaky I-SceI expression result in functional YFP. The panel shows the percentage of YFP<sup>+</sup> cells within the RFP<sup>-</sup> and RFP<sup>+</sup> fractions of each overnight-grown SSA-strain culture (n=4) as described in **(B)**. Bar heights and error bars correspond to mean and SEM (n=4) of YFP<sup>+</sup> percentages within the RFP<sup>+</sup> (n=4) and RFP<sup>-</sup> (n=4) fractions. Red points correspond to the percentages of YFP<sup>+</sup> cells in the individual cultures. RFP<sup>-</sup> fractions had a mean YFP<sup>+</sup> percentage of 99.2% indicating that the YFP reporter captures most SSA repair events. RFP<sup>+</sup> fractions had a mean YFP<sup>+</sup> percentage of 0.8% indicating that the YFP reporter is able to detect SSA repair even in cells in which RFP is not significantly diluted. **D.** Detection of YFP in nearly all cells following 4-hour doxycycline treatment of cultures. Data was obtained from the cultures prepared for the ‘Sequencing-based genotypic characterization of the SSA reporter activity’ (prior to flow-cytometer-facilitated cell-sorting) as described in the STAR Methods. Bar heights and error bars show the mean and SEM (n=3) of the YFP<sup>+</sup> percentages measured in the 3 cultures before and after doxycycline exposure. Red points correspond to YFP<sup>+</sup> percentage values measured in individual cultures. Prior to doxycycline addition, the mean percentage of YFP<sup>+</sup> cells was 4.6%. 9 hours after doxycycline introduction, the mean YFP<sup>+</sup> percentage was 99.8%.

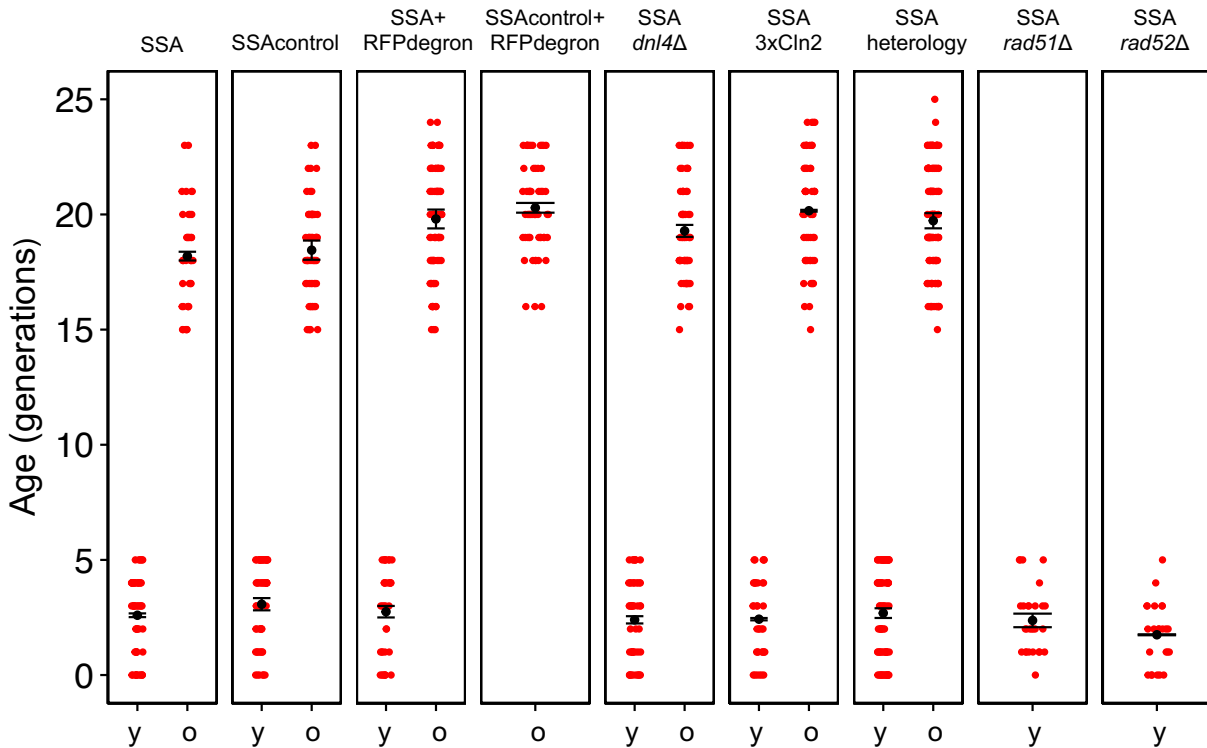


**Figure S4. Ages of cells at the beginning of doxycycline treatment for strains of the study, Related to Figures 2-5.** Error bars represent replicate-based mean $\pm$ SEM of replicative age (after averaging across cells in each replicate) at the beginning of the doxycycline treatment. Number of replicates (n) was equal to 2 for all strains/age-groups except SSA+RFPdegron old (n=3), and SSAheterology old (n=5). For both age groups, only cells that were alive 9 hours after doxycycline addition were considered (since these were the only cells used in the repair efficiency calculations). For the old-cell groups, only cells that were at least 15-generations old were included. y, young-cell group; o, old-cell group.

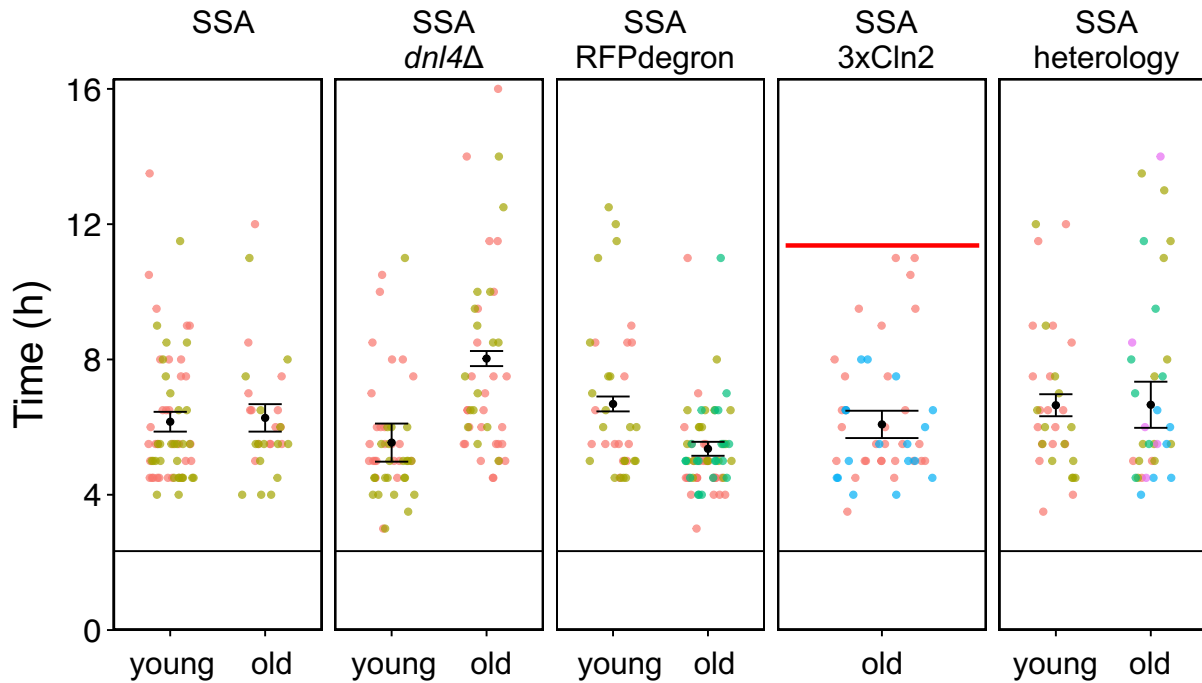


**Figure S5. YFP appearance times in the strains carrying the SSA repair reporter and its variants, Related to Figures 2C, 4A, 4C, 4F, 5A.** The y-axis indicates the time passed since the start of the fluorescence measurements in each movie. The black horizontal line with y-intercept at 2.3 h corresponds to the time of doxycycline addition relative to the start of the fluorescence measurements. For all SSA strains except the one with 3xCln2, fluorescence measurements were made up to 14 hours after doxycycline addition. For the strain with 3xCln2, fluorescence measurements were made up to 9 hours after doxycycline addition. The later missing measurement period is denoted by the time block above the red line. Points correspond to the time of first YFP appearance for individual cells. Error bars correspond to mean $\pm$ SEM ( $n=3$  for old SSA+RFPdegron,  $n=5$  for old SSA heterology,  $n=2$  for all other strain/age-group pairs) of the replicate averages (after averaging all cells' YFP appearance times in a replicate). Different colors correspond to different replicates.



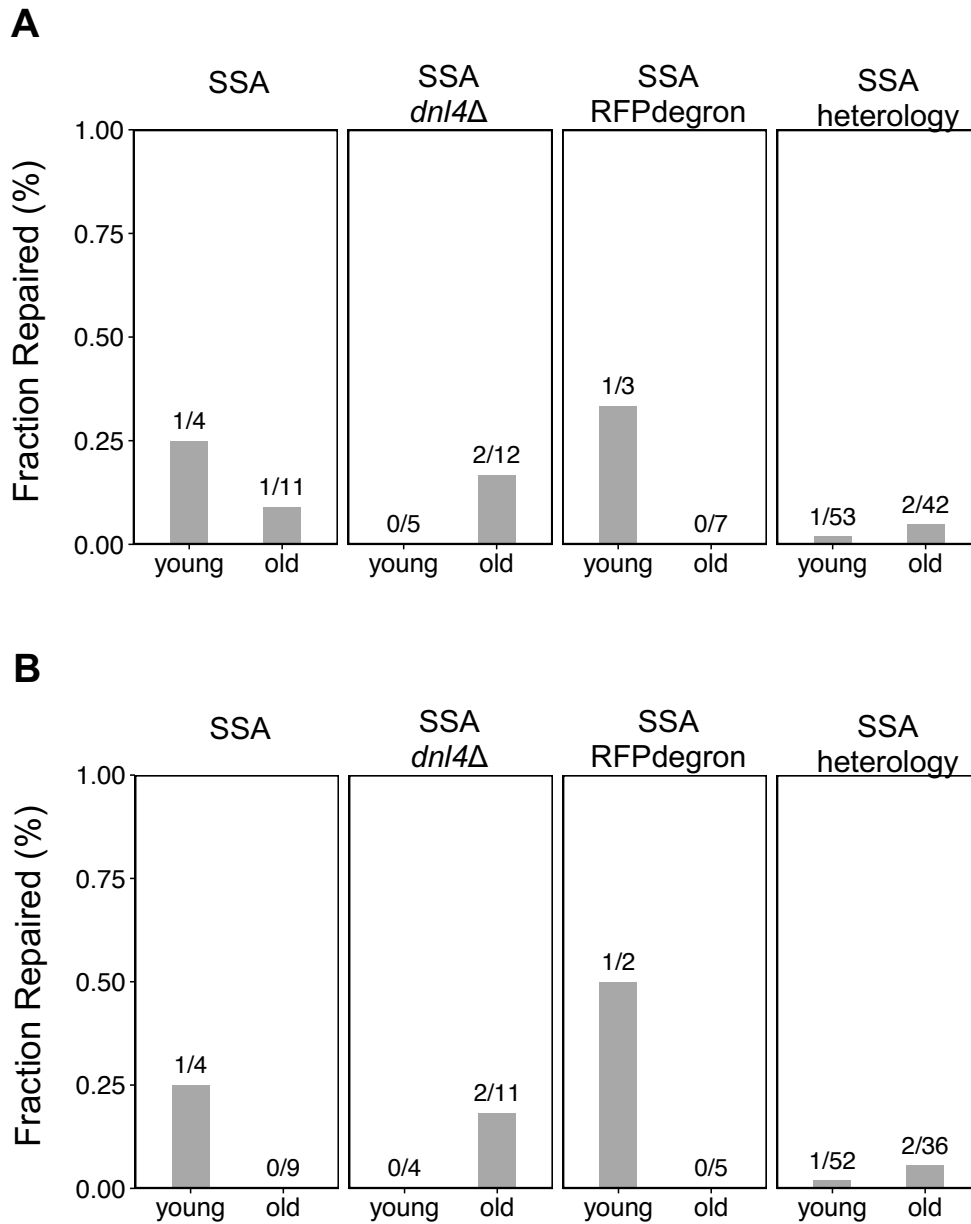


**Figure S6. Assessing SSA repair during the next 5 hours after the 9-hours post-doxycycline addition time window (only for cells unrepaired earlier). Related to Figures 2C, 4A, 4C, 5A.** Y-axis is the fraction of cells that were SSA unrepaired (YFP-) at the 9<sup>th</sup>-hour post-doxycycline addition time point but were repaired within the next 5 hours (between 9<sup>th</sup> hour and 14<sup>th</sup> hour time points after doxycycline addition). The cell counts used to compute these fractions are shown above the bars. **A.** Fraction of repair computed among cells that either burst in the 9h-14h time window, or were alive at the end of this window. **B.** Fraction of repair computed only among the cells that were alive at the end of the 9h-14h time window.

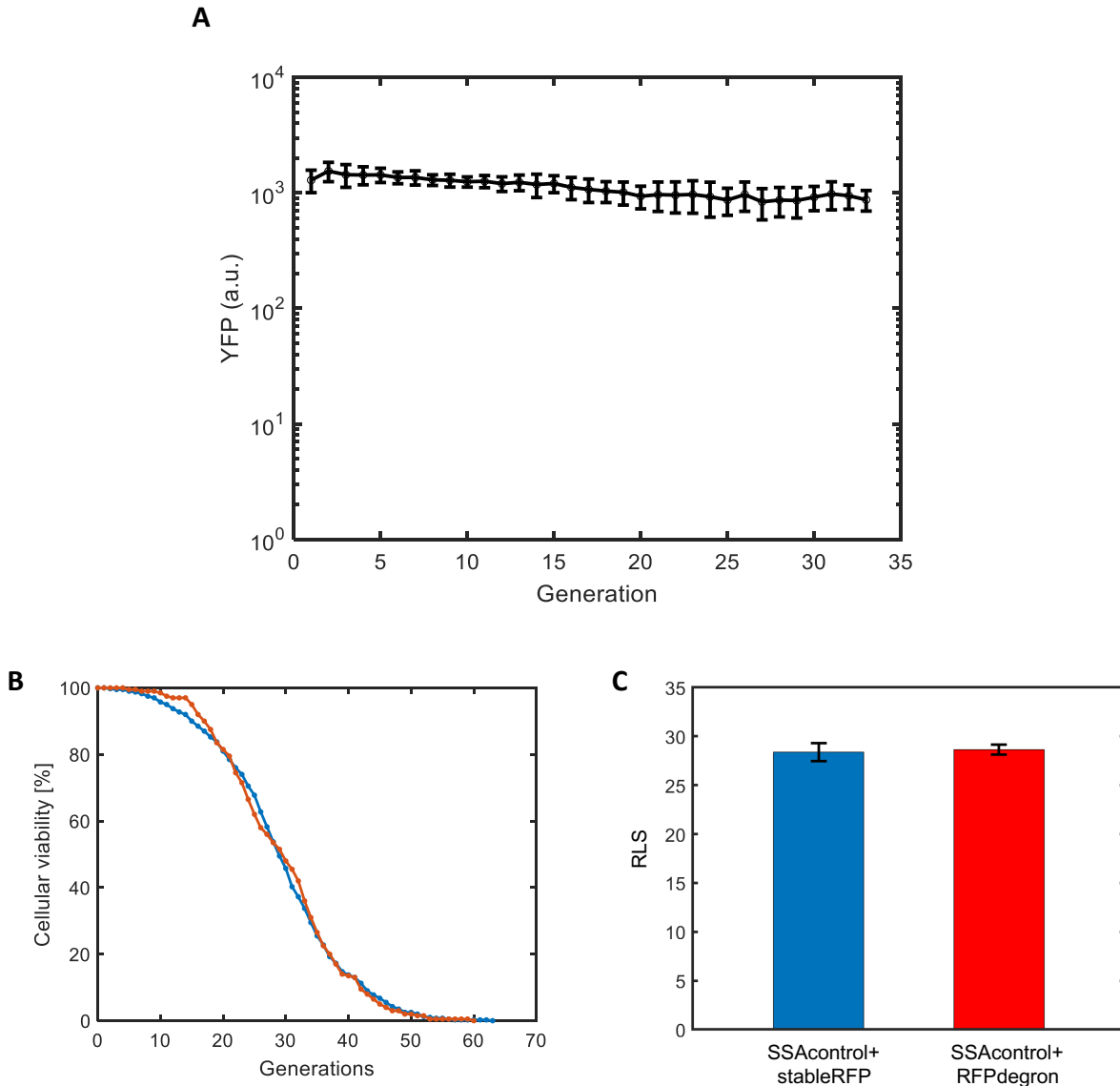


**Figure S7. A. Quantifying expression from  $P_{TEF1}$ -YFP during replicative aging, Related to Figure 1C.** A fluorescence measurement of a cell was assigned to generation  $x$  if it was the first fluorescence measurement to occur in the  $x^{\text{th}}$  generation window of that cell. The  $x^{\text{th}}$  generation window is the time between appearance of the  $x^{\text{th}}$  and  $(x+1)^{\text{th}}$  daughter bud. For each generation window, the mean and SD of the fluorescence measurements assigned to that window are plotted on a log scale. Only generation windows with at least 10 measurements are shown. **B-C. Replicative lifespan measurements using the SSA control strains (no cutsite) carrying stable RFP or degron-tagged RFP, Related to Figure 4C-E.** **B.** Cellular viability curves for the SSA control strains carrying stable RFP (blue) and degron-tagged RFP (red). 400 cells (4 biological replicates of

100 cells each) were used to generate the stableRFP strain's viability curve. 200 cells (2 replicates of 100 cells each) were used to generate the RFPdegren strain's viability curve. **C.** Using the data shown in **(B)**, mean $\pm$ -SEM of the replicate-based mean RLS measured for the two strains (n=4 replicates for stableRFP strain, and n=2 replicates for the RFPdegren strain).

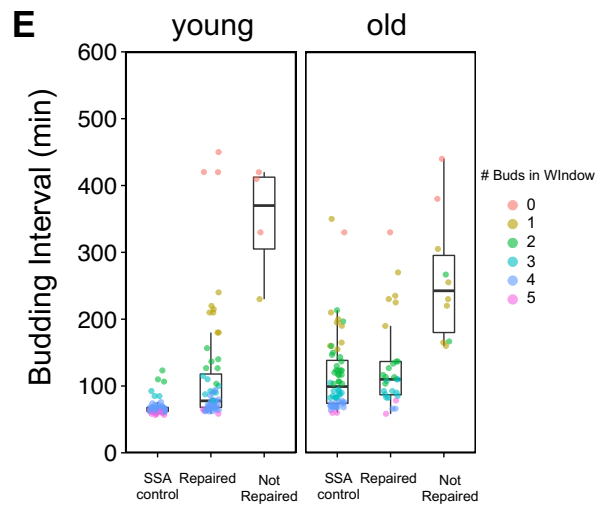
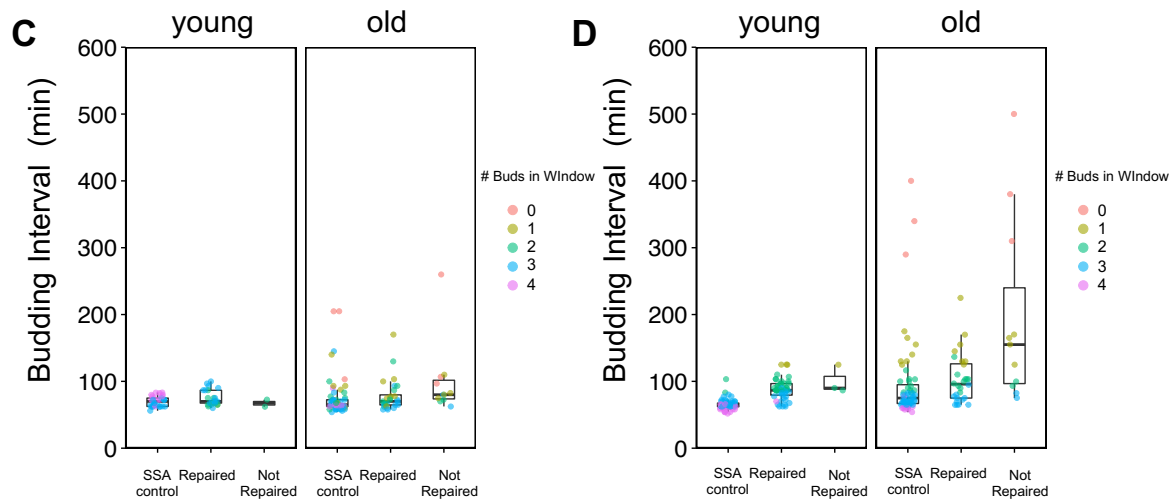
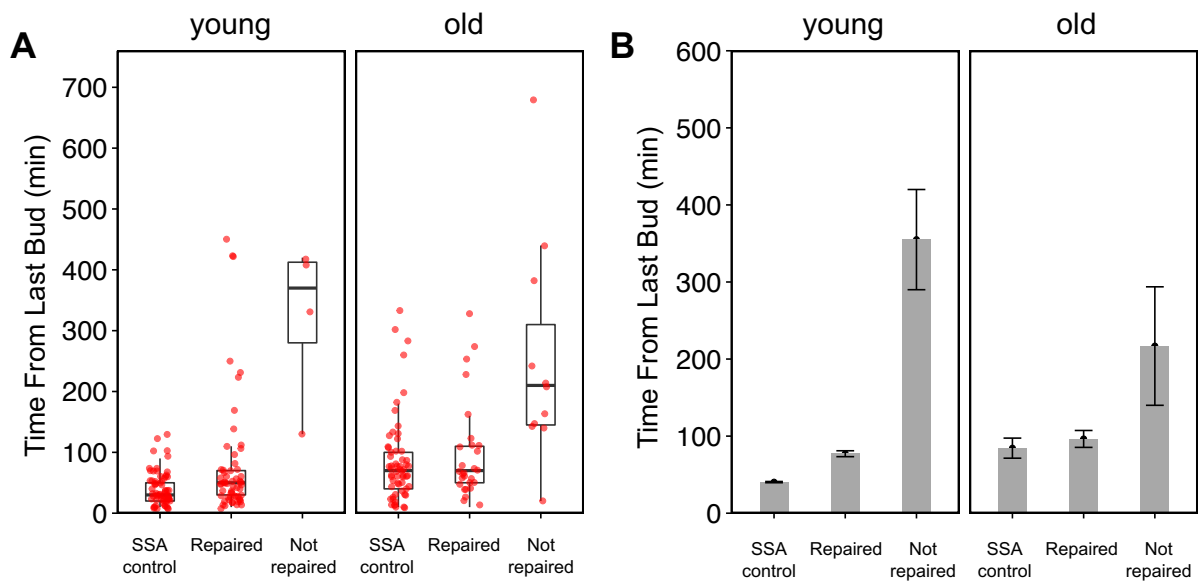


**Figure S8. A-B. Time from last bud measured at the 9<sup>th</sup> hour after doxycycline addition time point for cells carrying the SSA repair reporter cassette, Related to Figure 2.** For each age group (young vs old), cells are grouped by whether YFP was repaired at the end of the 9-hour post-doxycycline time window. Values for the SSA control strain are also shown for comparison. **A.** Values for individual cells from two replicates for each age group. Boxplots are overlaid to show the distribution of times for cells pooled across 2 replicates. **B.** Mean $\pm$ SEM (n=2) of average times from last bud (after averaging across all cells' times from last bud within each replicate). For both age groups, the unrepaired cells have a greater time from last bud at the 9<sup>th</sup> hour after doxycycline addition compared to the repaired cells (in the old case, 217 $\pm$ 77 min for the unrepaired cells vs 96 $\pm$ 11 min for the repaired cells). **C-E. Average budding intervals before (C), during (D), and after (E) the doxycycline treatment for repaired and unrepaired cells of the strain (yTY125a) containing the SSA repair reporter cassette, Related to Figure 2.** Individual data points correspond to average budding intervals for single cells. Single cell data pooled from 2 replicate experiments is shown, with boxplots for the distribution of values in each sub-group overlaid. **C.** During the 4-hour time window before doxycycline addition. **D.** During the 4-hour time window coinciding with doxycycline treatment. **E.** During the 5-hour time window after doxycycline removal.

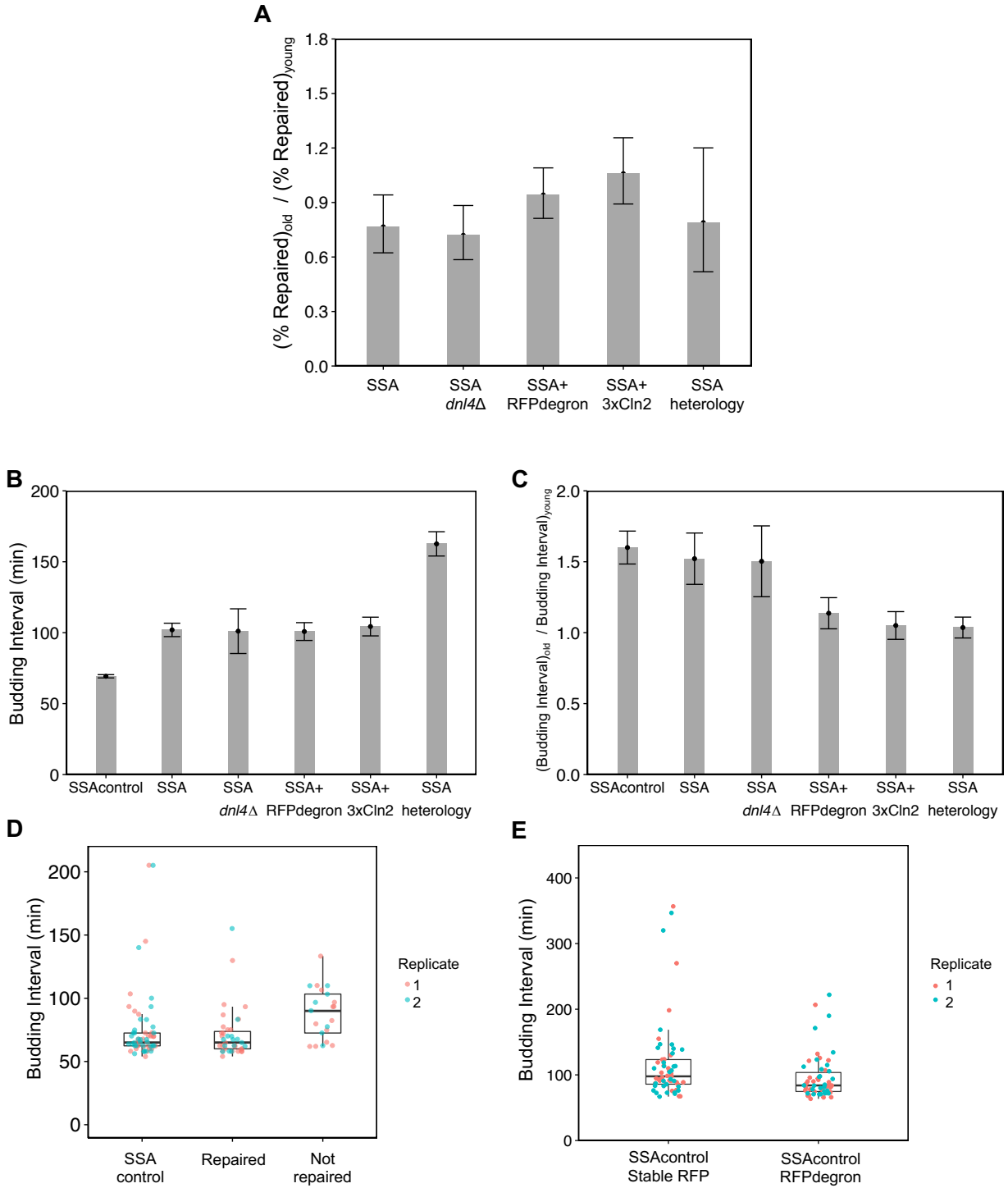


**Figure S9. A. Ratio of SSA repair efficiency in old cells to young cells of each strain, Related to Figures 2C, 4A, 4C, 4F, 5A.** Repair efficiency was defined as the fraction of cells repaired by SSA by the end of the 9-hours time window after doxycycline addition, so it is partly a measure of SSA repair speed.

For each strain shown, the ratio of the old cell repair efficiency to the young cell repair efficiency was taken. The error bars represent 95% confidence intervals based on applying the delta method to the log ratio of the pooled old cells' repaired fraction to the pooled young cells' repaired fraction (STAR Methods). The mean SSA repair efficiency ratio is greater for the SSA+RFPdegron and SSA+3xCln2 strains compared to the other three strains. The mean SSA repair efficiency ratios are: 0.77 for the SSA strain without the degron (yTY125a), 0.72 for the SSA strain lacking *DNL4* (yTY149a), 0.94 for the SSA+RFP degron strain (yTY147a), 1.06 for the SSA+3x*CLN2* strain (yTY161a), and 0.79 for the SSA strain with 3% heterology (yTY133c). **B-C. Strain-wise comparison of age-related slowdown in budding intervals during the 9-hour time window after doxycycline addition, Related to Figures 2D, 4B, 4D, 5B.** **B.** Average budding intervals during the 9-hour time window after doxycycline addition for young cells of each strain. Mean $\pm$ SEM of replicate-averaged single cell values for the time window are shown. **C.** Ratio of budding intervals between old and young cells of each strain, measured after doxycycline addition. For each cell, an average budding interval was calculated for the 9-hour time window after doxycycline addition. For each strain, the mean of replicate-averaged single-cell budding intervals was calculated for old-cell replicates and for young-cell replicates. Bar height corresponds to the ratio of these means. Error bars are calculated by propagating the uncertainty of each of the means. **D. Average budding intervals measured in the 4-hour pre-doxycycline time window for old cells of the strain containing the SSA reporter but lacking *DNL4* (yTY149b), Related to Figure 4A, 4B.** Individual points correspond to average budding intervals measured during the 4-hour pre-doxycycline time window for single cells. Cells are grouped by whether SSA repair was detected by YFP within the 9-hour time window after doxycycline addition. Budding intervals for the control strain lacking a cut-site are also shown for comparison. Boxplots for the distribution of the single cell values (pooled across the 2 replicates) are overlaid. **E. Average budding intervals measured after doxycycline addition for old cells of the SSAcontrol strains missing the cutsite, with stable RFP (yTY126a) or degron-tagged RFP (yTY146a), Related to Figure 4C-E.** Only cells of age 15 or older at the time of doxycycline addition were considered. All full-length budding intervals occurring at and after generation 15 were used. Points corresponding to average budding intervals (averaged for each single cell) during this time window are color coded by replicate. Boxplots for the distribution of the single cell values (pooled across the 2 replicates) are overlaid.

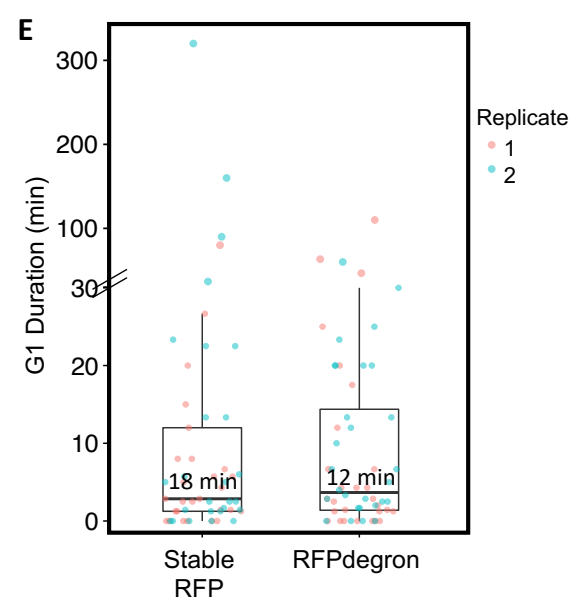
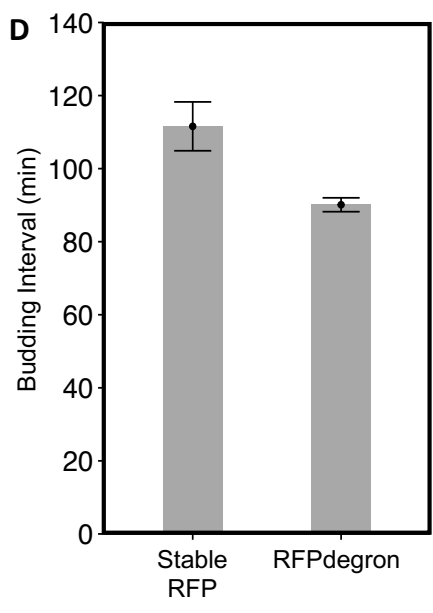
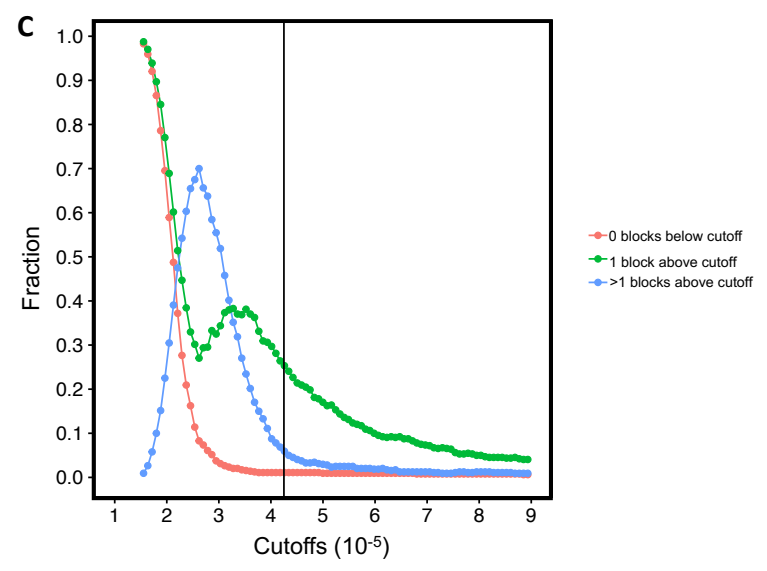
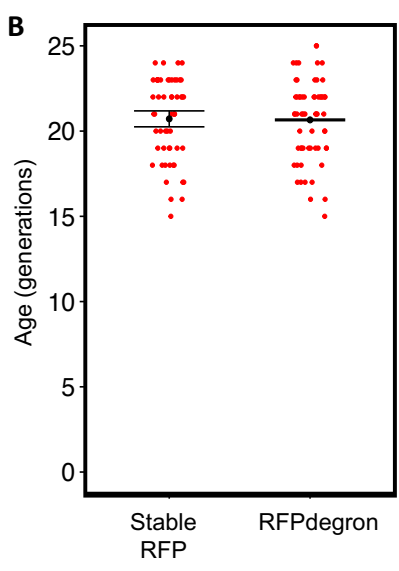
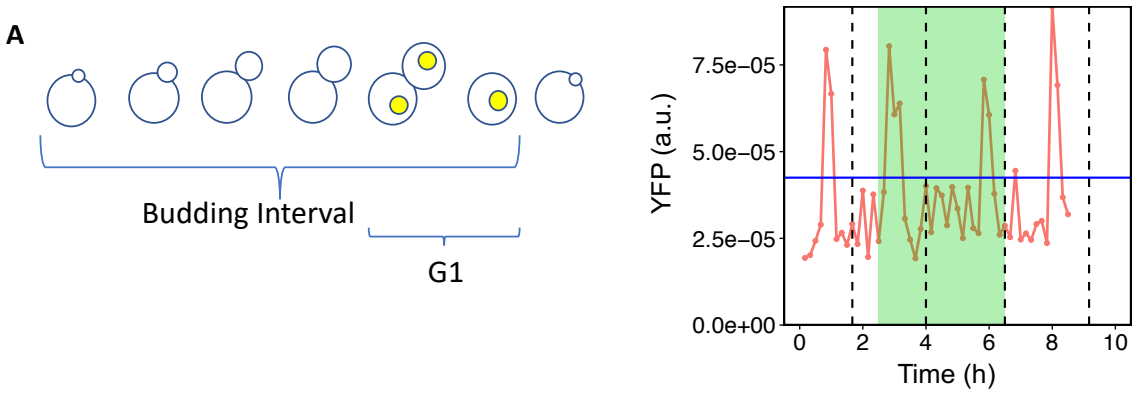




**Figure S10. Using Whi5-YFP localization to compare G1 duration in strains carrying the SSA control cassette with stable RFP or degron-tagged RFP, Related to Figure 4D-E.** **A.** Whi5-YFP localization was used to measure G1 duration. Whi5 enters the nucleus at the end of mitosis and remains there until the cell enters the next S phase (bud appearance). G1 durations were measured for each budding interval. For each cycle, the first appearance of each daughter bud was recorded. The time from first appearance of a daughter bud (inclusive) up to but not including the appearance of the next daughter bud was defined as the budding interval. The plot on the right shows how measurements of Whi5-YFP over time in a single cell are used to estimate G1 durations. Cells were aged using the same protocol as the experiments used to measure SSA efficiency in old cells. Green shading corresponds to the duration of doxycycline treatment. Bud appearances are the dashed vertical lines. For Whi5-YFP measurements within each budding interval, measurements were characterized relative to a cutoff (horizontal line). This divides the budding interval into blocks of measurements above or below the cutoff. For example, in the sample trajectory, the budding interval starting at 1.7 h and ending at 4 h, consists of a 'below', 'above', 'below' sequence of blocks. The pattern of blocks measured across many budding intervals is used to assess the quality of a YFP cutoff (**C**). Once a suitable cutoff was chosen, G1 duration for a budding interval was defined as the length of the longest block of measurements in the budding interval above the cutoff. **B.** Ages at the time of doxycycline addition for the Whi5-YFP containing cells used for measurement of G1 duration in the two strains. Only cells 15 generations or older at the time of doxycycline addition were used. Error bars show mean $\pm$ SEM (n=2) of replicate-based averages. Red points are ages of individual cells. Number of cells per replicate were 28 and 27 for the stable RFP strain, and 31 and 24 for the degron-tagged RFP strain. **C.** Assessment of various thresholds for Whi5-YFP localization. The data was obtained from 2 replicates each of the SSA control strains (no cut-site) carrying either the stable RFP or degron-tagged RFP. Whi5-YFP was measured for all budding intervals overlapping with the first 8.33 h of fluorescence measurements. For each threshold value, we determined the fraction of all budding intervals (pooled between the two strains) with 0 blocks (measurements) below the cutoff, exactly one block above the cutoff, and more than 1 block above the cutoff. Since Whi5 is nuclear-localized only during G1 and exits the nucleus prior to appearance of a bud, a suitable cutoff should yield a high fraction of budding intervals with exactly one block of time above the cutoff, and two blocks of time below the cutoff. Therefore, the fraction of budding intervals with 0 blocks below the cutoff, or more than 1 block above the cutoff should be low. Based on these criteria, a cutoff of 0.0000425 was chosen (vertical line). Using this cutoff value, the fraction of budding intervals with no

blocks below the cutoff, or too many blocks above the cutoff were both less than 10%. 620/626 (99%) of all budding intervals begin with a measurement below the cutoff. This is in agreement with Whi5 exit from the nucleus prior to bud appearance. **D.** Budding intervals measured in the two strains. For each cell, all budding intervals overlapping with the first 8.33 h of fluorescence measurements were averaged. The single cell average budding intervals were then averaged within each replicate. Bar heights and error bars are the mean $\pm$ SEM (n=2) of the replicate-based averages. **E.** G1 durations after applying the YFP cutoff of 0.0000425 described in (C) to data from the stable RFP and degron-tagged RFP strains containing the SSA control cassette (no cutsite). For each cell, G1 durations for the budding intervals overlapping with the first 8.33 h of fluorescence measurements were averaged. Budding intervals in which no measurements were above the cutoff were assigned a G1 duration of 0. Boxplots are displayed with single-cell G1 duration averages overlaid. The upper hinge is the 75<sup>th</sup> percentile, the middle line is the 50<sup>th</sup> percentile, and the lower hinge is the 25<sup>th</sup> percentile. The whiskers are drawn from each hinge to the most extreme data point less than or equal a distance of 1.5x the interquartile range from the hinge. Due to the high variation in the data, the scale is divided into two parts indicated by the hatchmarks on the y-axis at value 30. Above the hatch marks, the y-axis scale is squeezed to fit all of the outliers. The mean of all single-cell G1 durations (pooled from two replicates) is printed above the median line of each boxplot.

## II. Supplemental Tables and Legends

Percent YFP+	Percent RFP-	<i>TEF1</i> ... .... <i>P<sub>ADH1</sub></i> -RFP present ?	I-SceI cutsite	<i>URA3</i> locus- <i>P<sub>TEF1</sub></i> -YFP present?	Mutations in <i>P<sub>TEF1</sub></i> -YFP?	Number of Cultures	SSA?
>99%	>99%	no	NA	yes	NA	6	yes
0%	>99%	no	NA	yes	no start codon	3	yes
					TAG stop codon (193th bp of YFP)	6	yes
	0%	yes	deleted	no	NA	2	no
			intact	no	NA	1	no
1-10%	1-10%	yes	intact	no	NA	4	no

**Table S1. Results from the sequencing-based genotypic characterization of the SSA reporter activity, Related to Figure 1C.** See Figure S3A for a description of primers used for PCR amplification and sequencing. See the Key Resources Table for the primer sequences. See the STAR Methods section named ‘Sequencing-based genotypic characterization of the SSA reporter activity’, for a more detailed description of the results of the sequencing experiments.

Strain	Description	Genotype
yTY126a (‘SSAcontrol’ in figures)	SSA (control)	<i>MATα, his3Δ, LYS2, met15Δ, leu2Δ::LEU2-P<sub>MYO2</sub>-rtTA-Adh1t, ho::HIS5-P<sub>TETO4</sub>-l-Scel-Cyc1t, ura3Δ::URA3-SSAreporter(control, no cut-site)</i>
yTY125a (‘SSA’ in figures)	SSA (perfect homology)	<i>MATα, his3Δ, LYS2, met15Δ, leu2Δ::LEU2-P<sub>MYO2</sub>-rtTA-Adh1t, ho::HIS5-P<sub>TETO4</sub>-l-Scel-Cyc1t, ura3Δ::URA3-SSAreporter (perfect homology)</i>
yTY133c (‘SSAheterology’ in figures)	SSA (3% heterology)	<i>MATα, his3Δ, LYS2, met15Δ, leu2Δ::LEU2-P<sub>MYO2</sub>-rtTA-Adh1t, ho::HIS5-P<sub>TETO4</sub>-l-Scel-Cyc1t, ura3Δ::URA3-SSAreporter(with 3% heterology)</i>
yTY146a (‘SSAcontrol+ RFPdegron’ in figures)	SSA (control, RFPdegron)	<i>MATα, his3Δ, LYS2, met15Δ, leu2Δ::LEU2-P<sub>MYO2</sub>-rtTA-Adh1t, ho::HIS5-P<sub>TETO4</sub>-l-Scel-Cyc1t, ura3Δ::URA3-SSAreporter(control, no cut-site, with mCherry-ssCLN2PEST)</i>
yTY147a (‘SSA+ RFPdegron’ in figures)	SSA (RFPdegron)	<i>MATα, his3Δ, LYS2, met15Δ, leu2Δ::LEU2-P<sub>MYO2</sub>-rtTA-Adh1t, ho::HIS5-P<sub>TETO4</sub>-l-Scel-Cyc1t, ura3Δ::URA3-SSAreporter(perfect homology, with mCherry-ssCLN2PEST)</i>
yTY149b (‘SSA <i>dnl4Δ</i> ’ in figures)	SSA (perfect homology), <i>dnl4Δ</i>	<i>MATα, his3Δ, LYS2, met15Δ, leu2Δ::LEU2-P<sub>MYO2</sub>-rtTA-Adh1t, ho::HIS5-P<sub>TETO4</sub>-l-Scel-Cyc1t, ura3Δ::URA3-SSAreporter(perfect homology), dnl4Δ::KANMX4</i>
yTY159b (‘Stable RFP’ in Fig. S10)	SSA (control), Whi5 tagged to mCitrine	<i>MATα, his3Δ, LYS2, met15Δ, leu2Δ::LEU2-P<sub>MYO2</sub>-rtTA-Adh1t, ho::HIS5-P<sub>TETO4</sub>-l-Scel-Cyc1t, ura3Δ::URA3-SSAreporter(control, no cut-site), Whi5-mCitrine</i>
yTY160a (‘RFPdegron’ in Fig. S10)	SSA (control, RFP degron), Whi5 tagged to mCitrine	<i>MATα, his3Δ, LYS2, met15Δ, leu2Δ::LEU2-P<sub>MYO2</sub>-rtTA-Adh1t, ho::HIS5-P<sub>TETO4</sub>-l-Scel-Cyc1t, ura3Δ::URA3-SSAreporter(control, no cut-site, with mCherry-ssCLN2PEST), Whi5-mCitrine</i>
yTY161a (‘SSA 3xCln2’ in figures)	SSA (perfect homology), 3xCln2	<i>MATα, his3Δ, LYS2, met15Δ, leu2Δ::LEU2-P<sub>MYO2</sub>-rtTA-Adh1t, ho::HIS5-P<sub>TETO4</sub>-l-Scel-Cyc1t, ura3Δ::URA3-SSAreporter (perfect homology), CLN2::3xCLN2-KANMX4</i>
yTY164a (‘SSA <i>rad52Δ</i> ’ in Fig. S2)	SSA (perfect Homology), <i>rad52Δ</i>	<i>MATα, his3Δ, LYS2, met15Δ, leu2Δ::LEU2-P<sub>MYO2</sub>-rtTA-Adh1t, ho::HIS5-P<sub>TETO4</sub>-l-Scel-Cyc1t, ura3Δ::URA3-SSAreporter (perfect homology), rad52Δ::MET15</i>
yTY165a (‘SSA <i>rad51Δ</i> ’ in Fig. S2)	SSA (perfect Homology), <i>rad51Δ</i>	<i>MATα, his3Δ, LYS2, met15Δ, leu2Δ::LEU2-P<sub>MYO2</sub>-rtTA-Adh1t, ho::HIS5-P<sub>TETO4</sub>-l-Scel-Cyc1t, ura3Δ::URA3-SSAreporter (perfect homology) , rad51Δ::MET15</i>

**Table S2. Yeast strain descriptions and genotypes, Related to Figures 2-5.**

Strain Description	Age group at the start of dox treatment	Replicate	Number of cells used in repair efficiency calculation	Number of unrepaired cells at the start of dox treatment	Number of repaired cells at the start of dox treatment
SSA	young	1	33	39	1
SSA	young	2	31	31	3
SSA	old	1	21	31	4
SSA	old	2	18	29	6
SSAcontrol	young	1	21	22	0
SSAcontrol	young	2	44	44	0
SSAcontrol	old	1	30	41	0
SSAcontrol	old	2	31	38	0
SSA <i>rad52</i> Δ	young	1	11	17	0
SSA <i>rad52</i> Δ	young	2	13	17	0
SSA <i>rad51</i> Δ	young	1	13	14	4
SSA <i>rad51</i> Δ	young	2	15	17	3
SSAcontrol+RFPdegron	old	1	32	40	0
SSAcontrol+RFPdegron	old	2	26	32	0
SSA+RFPdegron	young	1	14	14	1
SSA+RFPdegron	young	2	23	24	3
SSA+RFPdegron	old	1	32	44	6
SSA+RFPdegron	old	2	23	41	5
SSA+RFPdegron	old	3	26	36	5
SSA <i>dnl4</i> Δ	young	1	25	25	3
SSA <i>dnl4</i> Δ	young	2	27	27	3
SSA <i>dnl4</i> Δ	old	1	38	44	5
SSA <i>dnl4</i> Δ	old	2	22	30	2
SSA 3xCln2	young	1	16	16	7
SSA 3xCln2	young	2	21	21	2
SSA 3xCln2	old	1	33	38	7
SSA 3xCln2	old	2	20	25	9
SSAheterology	young	1	46	48	0
SSAheterology	young	2	40	42	0
SSAheterology	old	1	20	42	0
SSAheterology	old	2	32	43	2
SSAheterology	old	3	21	33	1
SSAheterology	old	4	20	31	2
SSAheterology	old	5	16	28	0

**Table S3. Strains, age groups, and experimental replicates/cells used for SSA repair efficiency calculations, Related to Figures 2-5.** Column 6 refers to the cells that, at the beginning of doxycycline treatment, were both repaired (based on YFP) and in the appropriate age range. For a cell to be included in the repair efficiency calculation, it had to not only satisfy these conditions (column 5), but also be alive 5 hours after removal of doxycycline (column 4).